

Thermodynamics of switching in a multistable system

Jacob Cook^{1,2} and Robert G. Endres^{1,2,*}

¹*Department of Life Sciences, Imperial College, London SW7 2AZ, United Kingdom*

²*Centre for Integrative Systems Biology and Bioinformatics,
Imperial College, London SW7 2AZ, United Kingdom*

(Dated: September 6, 2022)

Multistable nonequilibrium systems are abundant outcomes of nonlinear dynamics with feedback but still relatively little is known about what determines the stability of the steady states and their switching rates in terms of entropy and entropy production. Here, we will link fluctuation theorems for the entropy production along trajectories with the action obtainable from the Freidlin–Wentzell theorem to elucidate the thermodynamics of switching between states in the large volume limit of multistable systems. We find that the entropy production at steady state plays no role, but the entropy production during switching is key. Additional stabilising and destabilising effects arise from the steady-state entropy and diffusive noise, respectively. The relevance to biology, ecological, and climate models is apparent.

When Niels Bohr and Erwin Schrödinger asked decades ago whether new physical principles are needed to explain living systems, the answer seemed No [1, 2]. More recently, however, the field of stochastic thermodynamics with its temporal violations of macroscopic thermodynamic laws at the microscopic scale have provided a new physical perspective on life. Most remarkable corner stones of far-from-equilibrium thermodynamics are the fluctuation theorems and Seifert’s thermodynamic uncertainty relation, stressing the important role of entropy production [3–6]. At equilibrium, detailed balance prohibits any entropy production on average, but far from equilibrium such entropy production is a characteristic feature [7] and determines the flow of time [8]. In particular, the fluctuation theorem by Evans and Searles allows the exact calculation of the entropy production along a trajectory from the time-forward and time-reversed path (corresponding to a movie played backwards), where paths can be calculated from e.g. Gillespie simulations of the underlying chemical master equation [4]. However, due to its intrinsic connection with the time-reversed path, it cannot be used to calculate the probability of a path simply from its entropy production. The situation is different when using the least-action principle, which allows the prediction of the most likely path between two points in a stochastic system from minimising the action (integral over the Lagrangian) [9, 10]. This is often done with a Langevin approximation of the master equation, such as using stochastic differential equations incorporating noise terms [11, 12]. However, now the link to thermodynamics is less clear as the role of the entropy production is obscured by the action functional.

In this letter, we combine the two to address the stability of steady states in non-equilibrium systems. In particular, we will elucidate the roles of steady-state entropy and fluctuations, as well as steady-state and path entropy production in state switching. For this purpose, we use two different low-dimensional minimal models shown in Fig. 1, the Schlögl [13] and the toggle switch [14] models,

for different far-from-equilibrium constraints — concentration clamping and flux constraints.

To investigate the thermodynamics of state switching we shall study bistable systems with macrostates denoted A and B , where both macrostates correspond to sets of microstates in the discrete space of molecule numbers \mathbf{X} , which is a vector for multiple chemical species. The assumption is made that no significant amount of time is spent outside these macrostates. In the large volume limit, the process of switching between states can be assumed to be a Poisson process (with exponentially distributed waiting times, see Fig. 1B inset). Thus, $\langle\tau_A\rangle = k_{A\rightarrow B} \int_0^\infty t \exp(-k_{A\rightarrow B}t) dt = k_{A\rightarrow B}^{-1}$ where $k_{A\rightarrow B}$ is the switching rate from A to B , and similarly for the B state. The occupation probability of the A state is then given by $p_A = \langle\tau_A\rangle / (\langle\tau_A\rangle + \langle\tau_B\rangle) = 1 / (1 + k_{A\rightarrow B} / k_{B\rightarrow A})$. Hence, such a two-state system is completely described by the ratio of the switching rates. How do we calculate these for actual molecular systems?

For non-equilibrium systems the dynamics can be described by a path Γ , e.g. $\mathbf{X}_0, \mathbf{X}_1, \mathbf{X}_2, \dots, \mathbf{X}_N$, obtainable from simulations of the chemical master equation [15]. For this time-forward path, there also exists a time-reversed path $\bar{\Gamma}, \mathbf{X}_N, \mathbf{X}_{N-1}, \dots, \mathbf{X}_0$. The probability of observing a particular path, e.g. the above time-forward path, is given by the path probability $P_\Gamma = \mathcal{N}P(\mathbf{X}_0)P(\tau_{0,1})W(\mathbf{X}_0|\mathbf{X}_1)\dots P(\tau_{N-1,N})W(\mathbf{X}_{N-1}|\mathbf{X}_N)$ assuming a memory-less Markov process with transition rates $W(\mathbf{X}_i|\mathbf{X}_{i+1})$. Furthermore, $P(\tau_{i,i+1})$ are probabilities for time intervals $\tau_{i,i+1}$ and \mathcal{N} is a normalisation factor, ensuring $\sum_\Gamma P_\Gamma = 1$. As we are considering a non-equilibrium steady state (NESS) probability distribution, the total change in entropy can be found from the steady-state fluctuation theorem (FT) [16] as

$$\Delta S_\Gamma = \ln(P(\mathbf{X}_0)/P(\mathbf{X}_N)) + \ln(W_\Gamma/W_{\bar{\Gamma}}), \quad (1)$$

with $W_\Gamma = W(\mathbf{X}_0|\mathbf{X}_1)\dots W(\mathbf{X}_{N-1}|\mathbf{X}_N)$ and $W_{\bar{\Gamma}} = W(\mathbf{X}_N|\mathbf{X}_{N-1})\dots W(\mathbf{X}_1|\mathbf{X}_0)$.

Restricting our consideration to paths that

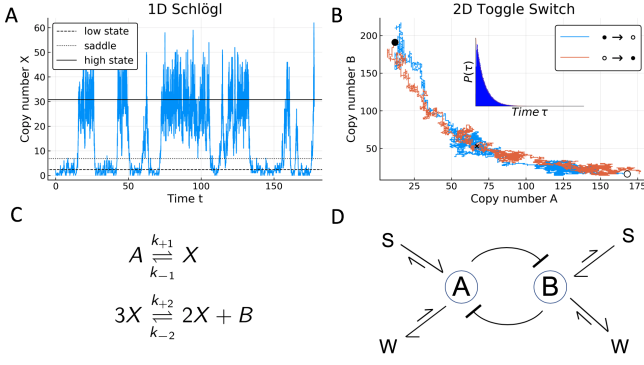


FIG. 1. **Overview of models.** (a) Example simulation of 1D (concentration clamped) Schlögl model, displaying switching between high and low X (copy number) states with A and B reservoir species held constant. (b) Example switching paths between A and B states for 2D toggle switch model. (Inset) Waiting time distribution for A to B switching, with a clear exponential distribution beyond a small initial time. (c) Symbolic chemical equations describing the Schlögl model. The flux constrained model will not be considered as bistability does not emerge. (d) Schematic illustration of 4 species toggle switch model, consisting of two mutually repressing chemical species (A, B) in addition to substrate (S) and waste (W) species. Further information on considered models and parameter values for example paths can be found in [21].

start within macrostate A and end within B , we can calculate the ensemble-averaged total entropy change $\Delta S_{A \rightarrow B} = \sum_{\Gamma|A \rightarrow B} P_{\Gamma} \Delta S_{\Gamma} = \langle \ln(P(\mathbf{X}_0)/P(\mathbf{X}_N)) \rangle_{A \rightarrow B} + \langle \ln(W_{\Gamma}/W_{\bar{\Gamma}}) \rangle_{A \rightarrow B}$, where the first term on the right-hand side (RHS) corresponds to the log ratio of steady-state probabilities of start $P(\mathbf{X}_0)$ and end $P(\mathbf{X}_N)$ points of the paths, weighted by the path probabilities from $A \rightarrow B$ (note N , \mathbf{X}_0 and \mathbf{X}_N can vary for different paths). Further, the second term on the RHS corresponds to the increase in entropy of the medium that the system is coupled to (here chemical reservoirs) [5]. In the limit of vanishing fluctuations (deterministic limit), the first term becomes negligibly small and the entropy produced is given by the second term only, e.g. $\Delta S_{A \rightarrow B} \approx \langle \ln(W_{\Gamma}/W_{\bar{\Gamma}}) \rangle_{A \rightarrow B} \approx \ln(k_{A \rightarrow B}/k_{\overleftarrow{A \rightarrow B}})$, with $k_{\overleftarrow{A \rightarrow B}}$ the rate associated with time-reversal of the most probable path (explained below) from A to B . When considering most probable switching paths, it is important to note that in general the time-reversed path does not describe the contrary switching path, i.e. $k_{\overleftarrow{A \rightarrow B}} \neq k_{B \rightarrow A}$ [17]. However, for simple enough systems, i.e. low dimensional systems, this approximation can be made, and switching rates are determined by entropy production as

$$k_{A \rightarrow B}/k_{B \rightarrow A} = \exp(\Delta S_{A \rightarrow B}). \quad (2)$$

Alternatively, we can make a continuum approximation of the master equation with the chemical Langevin equation, i.e. $X_i = x_i \Omega$ for $i = 1, \dots, K$ a K -dimensional

chemical system, with concentrations x_i and volume Ω . This is generally a reasonable approximation for large (but finite values) of Ω [18], particularly near equilibrium [19, 20]. However, while the accurate prediction of switching rates is difficult, the characterization of relative stability is easier. The chemical Langevin equation can be expressed as $\dot{x}_i = f_i(\mathbf{x}) + \Omega^{-1/2} g_{ij}(\mathbf{x}) \xi_j(t)$ with $\xi_j(t)$ uncorrelated white Gaussian noises of zero mean and autocorrelation $\langle \xi_i(t) \xi_j(t') \rangle = \delta_{ij} \delta(t - t')$. The deterministic force in direction i is given by f_i , and g_{ij} determines the propagation of noise from direction j to i . For the models considered in this paper g_{ij} is always diagonal. When the probability of escape from a macrostate is sufficiently improbable the stochastic transition will be expected to concentrate along a single path \mathbf{x}^* , with paths significantly diverging having probabilities so low (for large Ω) as to have negligible impact on overall escape probability [22]. The Wentzel-Kramers-Brillouin (WKB) approximation can then be used to obtain the probability of this path as $P_{A \rightarrow B} \sim \exp(-\Omega \mathcal{A}[\mathbf{x}^*])$, where $P_{A \rightarrow B}$ is the probability of transition from macro-state A to B , and \mathcal{A} is the action, as derived in [23]. The path \mathbf{x}^* will thus minimize the action $\mathcal{A}[\mathbf{x}^*] = \min \mathcal{A}[\mathbf{x}] = \mathcal{A}_{A \rightarrow B}$. The relevant action for a path with duration τ is the Freidlin-Wentzell (FW) action [23]

$$\mathcal{A}[\mathbf{x}] = \frac{1}{2} \int_0^{\tau} (\dot{\mathbf{x}} - \mathbf{f}) \mathbf{D}^{-1} (\dot{\mathbf{x}} - \mathbf{f})^T dt, \quad (3)$$

with the diffusion matrix given by $D_{ij} = g_{ik} g_{kj}^T$. This action can be considered a first order truncation of a more complete action, and once more terms are included switching paths no longer pass through the same saddle point as their converse [17]. The mean-first passage time (MFPT) is given by $T_{A \rightarrow B} \sim P_{A \rightarrow B}^{-1} = Q_{A \rightarrow B} \exp(\Omega \mathcal{A}_{A \rightarrow B})$ or $\ln(T_{A \rightarrow B}) = \ln(Q_{A \rightarrow B}) + \Omega \mathcal{A}_{A \rightarrow B}$, so that as Ω grows the contribution from the prefactor $Q_{A \rightarrow B}$ becomes less important and the second term on the RHS describes the MFPT to logarithmic precision.

An expression for entropy production based on the time-reversal of Langevin paths can be obtained by noting that the probability of the most probable switching path $A \rightarrow B$ is given by $P_{A \rightarrow B} = \exp(-\Omega \mathcal{A}_{A \rightarrow B})/Q_{A \rightarrow B}$. The probability of the corresponding time-reversed path $\overleftarrow{A \rightarrow B}$ is then found to be $P_{\overleftarrow{A \rightarrow B}} = \exp(-\Omega \mathcal{A}_{\overleftarrow{A \rightarrow B}})/Q_{A \rightarrow B}$, where $\mathcal{A}_{\overleftarrow{A \rightarrow B}}$ is the action of the time-reversed path. Combining the above two expressions as in Eq. 1 generates an expression for entropy production for Langevin paths as $\Delta S_{A \rightarrow B}^L = \Omega (\mathcal{A}_{\overleftarrow{A \rightarrow B}} - \mathcal{A}_{A \rightarrow B})$ [24]. Substituting Eq. 3 into this relation leads to

$$\Delta S_{A \rightarrow B}^L = 2\Omega \int_0^{\tau} \dot{x}_i D_{ij}^{-1} f_j dt. \quad (4)$$

Under the assumption that the ratios $k_{A \rightarrow B}/k_{B \rightarrow A}$ and $P_{A \rightarrow B}/P_{B \rightarrow A}$ approximately match, $\Delta S_{A \rightarrow B}$ and

$\Delta S_{A \rightarrow B}^L$ should be expected to return identical entropy production. However, the apparent entropy production from Eq. 4 disappears along with the action at steady state ($\dot{x}_i = f_i(\mathbf{x}) = 0$ in the small noise limit). This suggests that only entropy production along the path matters, and that the Langevin formalism within the steady state is equivalent to a quasi-equilibrium [21]. Despite the obvious difference between the master equation entropy production (Eq. 1) and the Langevin path entropy production (Eq. 4), there conceivably remains explanatory potential in the later. How does this entropy production vary along the path, and how do diffusion strength and steady-state entropies matter? Furthermore, does it matter how the non-equilibrium constraint is implemented? To answer these questions we introduce explicit minimal models.

The two models considered are the Schlögl and toggle switch models (Fig. 1). For both models concentration constraints are used to make the models non-equilibrium. Flux constrained models are not considered as the flux-constrained Schlögl model is not meaningfully bistable [21], and the flux-constrained toggle switch model is four-dimensional, and thus too computationally intensive for simulation of switches (mathematical details in [21]).

Figs. 2A,B show exemplar minimum action paths for switching in the Schlögl and the toggle switch model, respectively, calculated using the geometric minimum action method [21, 25–27]. The Schlögl model is sufficiently simple that the time-reversed switching paths correspond to the switching paths for the contrary direction. Fig. 2C shows how this leads to equal and opposite entropy productions (orange lines) along the paths. For the more complicated toggle switch model this simple relation between paths is lost, but Fig. 2D shows a linear relation between the difference in minimum action (purple line) and the difference in path entropy productions (gold line). Despite the systems' quasi-equilibrium behavior, non-equilibrium processes still occur. Figs. 2E,F show plots of the derived entropy production (EP, blue lines) and flow (EF, red lines), demonstrating non-zero contributions at the steady states (for full derivation see [21]).

In order to investigate links between occupation probabilities, entropy, and entropy production, 100 random parameters sets were created for each model (generated with constraints to avoid pathological cases, e.g., negative concentrations, degradation processes on average increasing copy numbers, etc.). Fig. 3A shows a weak correlation between state occupation probability and steady-state entropy production, which provides some evidence for the maximum entropy production principle (MaxEPP) [24]. This extremal principle proposes that states with higher entropy production are more dynamically stable (subject to other dynamical constraints) [28]. We then approximate the log ratio of state occupation probabilities via the Freidlin–Wentzell theorem as,

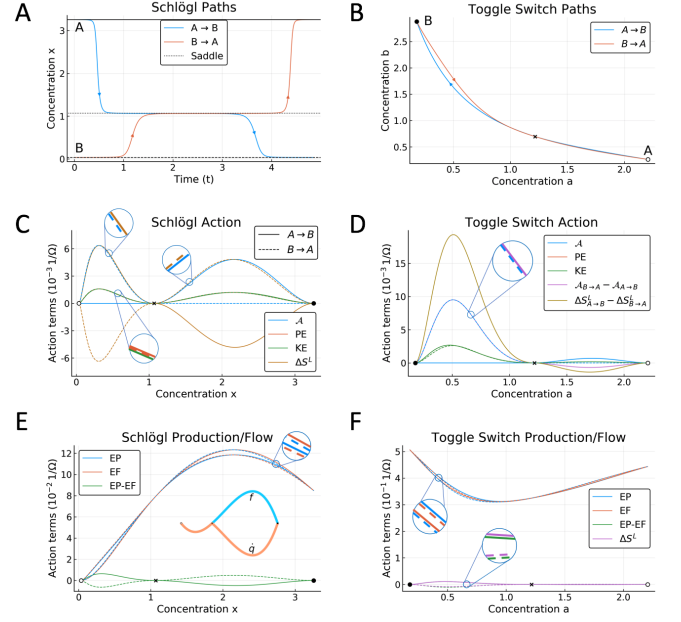


FIG. 2. Dependence of actions on path entropy productions. (a) Minimum action paths for Schlögl model; aside direction, the only difference between paths is the amount of time spent at the fixed points where there is no contribution to the action. (b) Minimum action paths for toggle switch model, now showing clear differences. (c) Action (\mathcal{A}), entropy production (ΔS^L), kinetic (KE) and potential energy (PE) of Schlögl paths, clearly showing that the entropy production of one path is the opposite of the other. In this and the remaining panels a solid line corresponds to the path from $A \rightarrow B$ and a dashed line to $B \rightarrow A$. Magnifications are meant to explain line styles. (d) Action, differences in action and entropy production, KE and PE along the toggle switch paths. The difference in action is proportional to the difference in entropy produced along the path (this linear relationship is further discussed below). (e) Entropy production (EP) and entropy flow (EF) terms along the Schlögl paths. The difference (EP-EF) is equal to the entropy production of time-reversed of Langevin paths. (Inset) Plot showing how f and \dot{x} vary along an exemplar minimum action path (see [21] for details). (f) Equivalent plot for the toggle switch paths.

$\ln(p_A/p_B) \approx \ln(P_{B \rightarrow A}/P_{A \rightarrow B}) = \ln(Q_{B \rightarrow A}/Q_{A \rightarrow B}) + \Omega(\mathcal{A}_{A \rightarrow B} - \mathcal{A}_{B \rightarrow A})$. For large Ω only the second term would be expected to contribute but this limit is difficult to simulate. Simulated occupation probabilities match well with this approximation (see Fig. 3B), demonstrating the validity of our use of the FW action. Fig. 3C shows a weak correlation between difference in action and difference in state entropy, as expected from equilibrium theory where higher entropy states are more stable. However, state entropy increases sublinearly with Ω so for large Ω it has no effect on the stability. Fig. 3D shows a comparison of the difference in action and the difference in path entropy production, showing that the linear relation observed in Fig. 2C,D holds generally across parameter sets surveyed. The effect of diffusion strength

was found to be minimal, and is therefore provided in [21].

Our results suggest a limited form of the MaxEPP, which applies to the rate of switching between macrostates. We shall proceed with our derivation by noting that the action can be split into two parts as $\Omega \mathcal{A}_{A \rightarrow B} = \mathcal{C}_{A \rightarrow B} - \frac{1}{2} \Delta S_{A \rightarrow B}^L$, where $\mathcal{C}_{A \rightarrow B}$ is the conservative action along the path $A \rightarrow B$ and $\Delta S_{A \rightarrow B}^L$ is the Langevin path entropy production (Eq. 4) [24]. The conservative action can be expressed in a similar form to Eq. 4 as

$$\mathcal{C}_{A \rightarrow B} = \frac{\Omega}{2} \int_0^\tau (\dot{x}_i D_{ij}^{-1} \dot{x}_j + f_i D_{ij}^{-1} f_j) dt, \quad (5)$$

where the two terms resemble kinetic and potential energy contributions, respectively. By substituting the expanded form of the action into the expression for switching path probability, a reduced form of MaxEPP can be obtained

$$P_{A \rightarrow B} = \frac{\exp(\frac{1}{2} \Delta S_{A \rightarrow B}^L - \mathcal{C}_{A \rightarrow B})}{Q_{A \rightarrow B}}, \quad (6)$$

where $P_{A \rightarrow B}$ is the probability of the (most probable) switching path along $A \rightarrow B$, and $Q_{A \rightarrow B}$ is a constant. This equation shows that there is a trade-off between minimization of the conservative action (i.e. fulfilling the equation of motion) and maximization of the path entropy production (i.e. being as dissipative as possible).

Generally, the switching path and its contrary path are travelled with the same speed and pass through similar regions of space. Thus, they are expected to have similar conservative actions (i.e. $\mathcal{C}_{A \rightarrow B} \approx \mathcal{C}_{B \rightarrow A}$). This relation is exact in the limit of matching time-reversed and converse switching paths (i.e. $\overline{A \rightarrow B} = B \rightarrow A$), which is the case for the Schlögl model. This expectation does not extend to the dissipative (path entropy production) component Eq. 4, as this depends on the cross terms of velocity $\dot{\mathbf{x}}$ and deterministic force \mathbf{f} , and so the velocity with which a region of space is passed matters. Hence, the entropy production components are not expected to cancel upon subtraction. An analytic relation can then be obtained as

$$\frac{1}{2} (\Delta S_{B \rightarrow A}^L - \Delta S_{A \rightarrow B}^L) \approx \Omega (\mathcal{A}_{A \rightarrow B} - \mathcal{A}_{B \rightarrow A}) \quad (7)$$

in line with expectation from the FT (Eq. 2, see [21] for details). In the toggle switch model where $A \rightarrow B \neq \overline{B \rightarrow A}$ this relation still holds for the majority of parameterizations, as can be seen in Fig. 3D. Significant divergence from the relation was generally observed in cases where the saddle point occurred at a low copy number compared to the steady states, due to the substantially faster variation of the force in low-copy-number regions (see [21]).

There has been significant interest in the thermodynamics of the transition between different steady-state probability distributions when controlled by an external

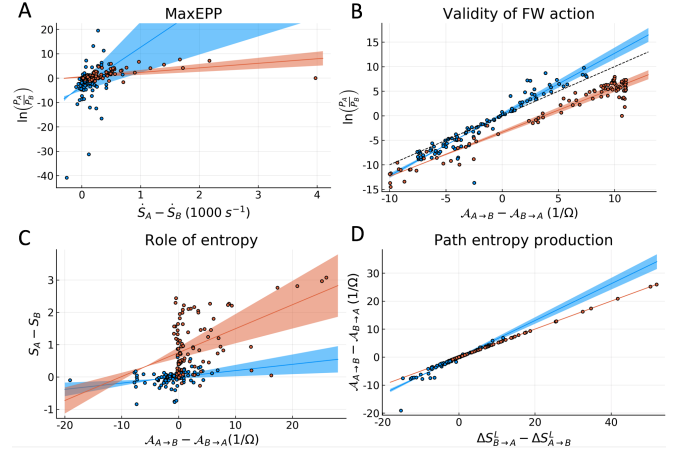


FIG. 3. Comparison of states and switching paths. In all panels, red and blue dots denote specific parameterizations of Schlögl and toggle switch models, respectively. In each plot the lines and shaded regions indicate best fits and 95% confidence intervals for the particular data sets, respectively. (a) Comparison of log ratios of occupation probabilities vs difference in entropy productions at steady states from Gillespie simulations. The Schlögl data has a Pearson correlation of 0.5172 and the toggle switch has 0.3476. (b) Log ratio of occupation probabilities obtained from Gillespie simulation vs the difference in minimum action. The dashed line indicates a perfect correspondence. The toggle switch and Schlögl data have correlations of 0.9515 and 0.9738, respectively. The results shown are coarsely discretized due to the low Ω used to save computational time. The discretization will effect the Schlögl B state disproportionately as it is formed of significantly fewer microstates than A . This represents a potential explanation for the downwards shift of the Schlögl data. (c) Comparison of difference in entropy of steady states vs difference in action. Entropies were found by Gillespie simulation with $\Omega = 1$. Both sets of data show weak correlations of 0.2892 and 0.4622 for the Schlögl and toggle switch models, respectively. (d) Difference in action vs difference in entropy produced along paths. Both models display a strong linear relationship, with correlations of 0.9445 and 1.0000 for the toggle switch and Schlögl models, respectively.

parameter [29, 30]. This is fundamentally different to our work, which is about the thermodynamics of switching between metastable states. In our two-state systems, we would naively expect a net zero entropy production through switching as the entropy produced by a switch in one direction would be cancelled by the eventual switch back. Only in cases where the switching path differs from the converse switching path are there net fluxes of probability through the system and thus entropy production. Consistently, for the Schlögl model we find no net entropy production (i.e. $\Delta S_{A \rightarrow B}^L = -\Delta S_{B \rightarrow A}^L$). In [31], bounds on the ratio of transition rates between two metastable states based on relative entropy ΔH and path entropy production are found. This ratio is determined as $\pi(B \rightarrow A)/\pi(A \rightarrow B) \geq \exp[-\Delta S_{A \rightarrow B}]$, where $\pi(A \rightarrow B)$ is the sum of the rates of switching A to B

over all possible switching channels. With the expectation that a single most probable path will dominate, consideration of the two contrary switching paths will be sufficient. Combining the main result of their paper with our analytic relation (Eq. 7) leads to a bound on the path entropy produced as $\Delta S_{A \rightarrow B}^L + \Delta S_{B \rightarrow A}^L \geq 0$, which becomes an equality in the limit of time-reversed switching paths (e.g. Schlögl). Every parameter set used in Fig. 3 was found to satisfy this condition. Beyond the physics literature, related frameworks to ours have been used in evolutionary science [32] where cumulative fitness flux is maximized (like entropy production) subject to the trade-off that speed of allele change and magnitude of selective forces are minimized (like the conservative action). Our results therefore suggest, that states in evolutionary systems that require greater cumulative fitness fluxes to reach should be expected to be more stable.

Our primary conclusion is that a MaxEPP for switching paths can be obtained within the Langevin approximation (Eq. 6), extending the rule that “exergonic reactions occur spontaneously” to switching in multistable systems. In a system with a large number of potential macrostates our relation predicts that for sufficiently large volumes switches that produce more entropy will be favoured. If regions of state space with greater entropy productions also require greater path entropy productions to reach, then this could form a basis for a more extensive maximum entropy production principle. Our secondary conclusion is that there exists a relationship between the difference in action of minimum action paths and difference in entropy produced along these paths (Eq. 7), valid for all paths that do not pass through regions of rapidly varying force. Exploring the application of our theory in ecology and evolutionary science with multiple stable states will be an interesting way forward [33].

Acknowledgements: J.C. and R.G.E. thankfully acknowledge helpful discussions with Shamil Chandaria, Henrik Jensen, Chiu Fan Lee, Gunnar Pruessner, David Schnoerr, Philipp Thomas, and financial support from the NERC CDT in Quantitative and Modelling Skills in Ecology and Evolution, and BBSRC grant BB/N00065X/1.

* E-mail: r.endres@imperial.ac.uk

- [1] N. Bohr, *Nature* **131**, 421 (1933).
- [2] E. Schrödinger, *What is Life? The Physical Aspect of the Living Cell* (Cambridge University Press, 1944).
- [3] D.J. Searles and D.J. Evans *Phys. Rev. E* **60**, 159 (1999).
- [4] D.J. Evans and D.J. Searles, *Advan. Phys.* **51**, 1529 (2002).

- [5] U. Seifert, *Rep. Prog. Phys.* **75**, 126001 (58pp) (2012).
- [6] A.C. Barato and U. Seifert, *Phys. Rev. Lett.* **114**, 158101 (2015).
- [7] C. Battle, C.P. Broedersz, N. Fakhri, V.F. Geyer, J. Howard, C.F. Schmidt, F.C. MacKintosh, *Science* **352**, 604 (2016).
- [8] É. Roldán, I. Neri, M. Dörpinghaus, H. Meyr, F. Jülicher, *Phys. Rev. Lett.* **115**, 250602 (2015).
- [9] M. Assaf and B. Meerson, *J. Phys. A: Math. Theor.* **50**, 263001 (2017).
- [10] P. Arnold, *Phys. Rev. E* **61** 6099 (2000).
- [11] R. Perez-Carrasco, P. Guerrero, J. Briscoe, K.M. Page, *PLoS Comput. Biol.* **12**, e1005154 (2016).
- [12] R. de la Cruz, R. Perez-Carrasco, P. Guerrero, T. Alarcon, K.M. Page, *Phys. Rev. Lett.* **120**, 128102 (2018).
- [13] F. Schlögl, *Z. Physik.* **253**, 147 (1972); M. Vellela and H. Qian, *J. Roy. Soc. Interface* **6**, 925 (2009); R.G. Endres, *PLoS One*, **10**, e0121681 (2015).
- [14] J.L. Cherry and F.R. Adler, *J. Theor. Biol.* **203**, 117 (2000).
- [15] P. Gaspard, *J. Chem. Phys.* **120**, 8898 (2004).
- [16] U. Seifert, *Phys. Rev. Lett.* **95**, 040602 (2005).
- [17] H. Feng, K. Zhang, J. Wang, *Chem. Sci.* **5**, 3761 (2014).
- [18] D.T. Gillespie, *J. Chem. Phys.* **113**, 297 (2000).
- [19] R. Grima, P. Thomas, A.V. Straube, *J. Chem. Phys.* **135** 084103 (2011).
- [20] P. Hanggi, H. Grabert, P. Talkner, H. Thomas, *Phys. Rev. A* **29** 371 (1984).
- [21] See Supplemental Material at [URL will be inserted by publisher] for extended description of models, details of numerical methods used and extended derivation of results.
- [22] H. Touchette, *Phys. Rep.* **478**, 1 (2009).
- [23] A.D. Ventsel and M.I. Freidlin, *Russ. Math. Surv.* **25**, 1 (1970).
- [24] R.G. Endres, *Sci. Rep.* **7**, 14437 (2017).
- [25] M. Heymann and E. Vanden-Eijnden, *Phys. Rev. Lett.* **100**, 140601 (2008).
- [26] M. Heymann and E. Vanden-Eijnden, *Commun. Pure Appl. Math.* **61**, 1052 (2008).
- [27] J.C. Neu, A. Ghanta, S. Teitworth, in *Coupled Mathematical Models for Physical and Biological Nanoscale Systems and Their Applications*, (Springer International Publishing, 2018), pp. 153-167.
- [28] R. Dewar, *Entropy* **11**, 931 (2009); R.D. Lorenz, J.I. Lunine, P.G. Withers, C.P. McKay, *Geophys. Res. Lett.* **28**, 415 (2001).
- [29] T. Hatano and S.I. Sasa, *Phys. Rev. Lett.* **86**, 3463 (2001).
- [30] G.B. Bagci, U. Tirnakli, J. Kurths, *Phys. Rev. E* **87**, 032161 (2013).
- [31] D. Ruelle, *J. Stat. Phys.* **164**, 463 (2016).
- [32] H.P. de Vladar and N.H. Barton, *Trends Ecol. Evol.* **26**, 424 (2011); V. Mustonen and M. Lässig, *PNAS* **107**, 4248 (2010).
- [33] M. Scheffer, J. Bascompte, W.A. Brock, V. Brovkin, S.R. Carpenter, V. Dakos, H. Held, E.H. van Nes, M. Rietkerk, G. Sugihara, *Nature* **461**, 53 (2009).
- [34] J. Schnakenberg, *Rev. Mod. Phys.* **48**, 571 (1976).
- [35] D.T. Gillespie, *J. Phys. Chem.* **81**, 2340 (1977).
- [36] J. Mehl, B. Lander, C. Bechinger, V. Blickle, U. Seifert, *Phys. Rev. Lett.* **108**, 220601 (2012).